J. Membrane Biol. 207, 91–105 (2005)
DOI: 10.1007/s00232-005-0804-1

The Journal of
Membrane
Biology

Contrasting Effects of Cd^{2+} and Co^{2+} on the Blocking/Unblocking of Human Ca_v3 Channels

D. Díaz, R. Bartolo, D.M. Delgadillo, F. Higueldo, J.C. Gomora
Departamento de Biofisica, Instituto de Fisiologia Celular, Universidad Nacional Autonoma de Mexico, Mexico City, DF 04510, Mexico

Received: 10 May 2005/Revised: 10 October 2005

Abstract. Inorganic ions have been used widely to investigate biophysical properties of high voltage-activated calcium channels (HVA: Ca_v1 and Ca_v2 families). In contrast, such information regarding low voltage-activated calcium channels (LVA: Ca_v3 family) is less documented. We have studied the blocking effect of Cd^{2+}, Co^{2+} and Ni^{2+} on T-currents expressed by human Ca_v3 channels: $Ca_v3.1$, $Ca_v3.2$, and $Ca_v3.3$. With the use of the whole-cell configuration of the patch-clamp technique, we have recorded Ca^{2+} (2 mM) currents from HEK−293 cells stably expressing recombinant T-type channels. Cd^{2+} and Co^{2+} block was 2- to 3-fold more potent for $Ca_v3.2$ channels (EC_{50} = 65 and 122 μM, respectively) than for the other two LVA channel family members. Current-voltage relationships indicate that Co^{2+} and Ni^{2+} shift the voltage dependence of $Ca_v3.1$ and $Ca_v3.3$ channels activation to more positive potentials. Interestingly, block of those two Ca_v3 channels by Co^{2+} and Ni^{2+} was drastically increased at extreme negative voltages; in contrast, block due to Cd^{2+} was significantly decreased. This unblocking effect was slightly voltage-dependent. Tail-current analysis reveals a differential effect of Cd^{2+} on $Ca_v3.3$ channels, which can not close while the pore is occupied with this metal cation. The results suggest that metal cations affect differentially T-type channel activity by a mechanism involving the ionic radii of inorganic ions and structural characteristics of the channels pore.

Key words: Ca_v3 — Unblocking — Cadmium — Cobalt — Nickel

Introduction

Calcium influx through voltage-dependent Ca^{2+} channels is crucial for many cellular functions, including neuronal excitability, muscle contraction, secretion of hormones and neurotransmitters, cell differentiation and gene expression (Bootman, Lipp & Berridge, 2001). The importance of these channels is also clinically relevant because Ca^{2+} channels are important pharmacological targets in the treatment of pain, hypertension, and certain forms of epilepsy (Mitterdorfer et al., 1998; Kim et al., 2001; Todorovic et al., 2001a, 2001b) and have been therefore subjected to intense research. However, such an effort has been focused mainly on high voltage-activated Ca^{2+} channels (HVA), and just recently the other members of the family, the low voltage-activated Ca^{2+} channels (LVA or T-type) have been object of such studies. One area that has received considerable interest is the use of inorganic ions (mainly divalent and trivalent metal ions) for analyzing function and structure of Ca^{2+} channels. Because metal ions are simple, have well-characterized atomic structures, and show small size differences, all of which are important for probing permeability mechanisms, they are a powerful tool to study the biophysical properties of Ca^{2+} channels (Elinder & Arhem, 2003).

Previous studies of Ca^{2+} channel block by metal cations have provided valuable insights into HVA-channel structure and function (Nachshen, 1984; Lansman, Hess & Tsien, 1986; Chow, 1991; Wakamori et al., 1998). Recently, with the cloning of three different α_1 subunits that express T-type calcium currents (Cribbs et al., 1998; Perez-Reyes et al., 1998; Lee et al., 1999a), there have been considerable advances in the understanding of how inorganic ions interact with LVA channels. With the advantage of having isolated currents (free of contamination by other channels' activity) when using recombinant Ca^{2+} channels, several work groups have now reported some important clues about the actions of

Present address for R. Bartolo: Facultad de Biología, Universidad Michoacana de San Nicolás de Hidalgo, Morelia, 58040, Mexico
Correspondence to: J.C. Gomora; email: jgomora@ifc.unam.mx

inorganic ions on T-type channels. First, $Ca_v3.2$ (α_{1H}) has been shown to be selectively blocked by low micromolar concentrations of Ni^{2+}, Cu^{2+} and Zn^{2+}, while $Ca_v3.1$ (α_{1G}) and $Ca_v3.3$ (α_{1I}) channels require 20- to 200-fold higher concentrations to induce the same effect (Lee et al., 1999b; Jeong et al, 2003). Also, studies with trivalent metal ions have demonstrated that Y^{3+} is the most potent inhibitor of $Ca_v3.1$ channels (Beedle, Hamid & Zamponi, 2002), although the sensitivity of the other two members of Ca_v3 channels to these inorganic ions has not been reported. Notably, by using Y^{3+} as a tool, it was suggested that the primary activation gate of $Ca_v3.1$ must be in the intracellular side of the selectivity filter (Obejero-Paz, Gray & Jones, 2004).

As a further examination for actions of divalent metal ions on Ca_v3 channel activity, we have used the three members of the human LVA channel family cloned to date (i.e., $Ca_v3.1$, $Ca_v3.2$, and $Ca_v3.3$), to improve our knowledge about the blocking effects of Cd^{2+}, Co^{2+} and Ni^{2+}, with particular interest in the modifications promoted by extreme potentials on the effects of the inorganic antagonists. We found $Ca_v3.2$ channels to be the ones most sensitive to block by Cd^{+} and Co^{2+}, although the voltage-dependent effects were observed mainly in $Ca_v3.1$ and $Ca_v3.3$ channels. Interestingly, repolarization to extreme negative potentials elicited opposite effects on Ca_v3 channels blocked by Cd^{2+} compared with those blocked by Co^{2+} and Ni^{2+}. This result indicates that metal cations affect T-type channel activity by different mechanisms. Additionally, our results about the effect of Cd^{2+} on $Ca_v3.3$ tail currents suggest that the channel can not close while the pore is occupied by the divalent cation.

Materials and Methods

Cell Culture

HEK-293 cells stably transfected with human $Ca_v3.1$ (α_{1G}; GenBank accession number AF190860; (Cribbs et al., 2000); $Ca_v3.2$ (α_{1H}; GenBank accession number AF051946, Cribbs et al., 1998); and $Ca_v3.3$ (α_{1I}; GenBank accession number AF393329, Gomora et al., 2002), were kindly provided by Dr. E. Perez-Reyes. Cell lines were cultured in Dulbecco's modified Eagle's medium (DMEM) supplemented with 10% fetal bovine serum, 100 U ml^{-1} penicillin, and 100 μg ml^{-1} streptomycin, and kept in a CO_2 incubator at 37°C. Selection of cells expressing the channels was maintained by adding 1 mg ml^{-1} G-418 to the culture medium. Once every 4–5 days the maintenance cultures were split by using a brief trypsin digestion in a Ca- and Mg-free saline (Trypsin-EDTA) to detach the cells, followed by mechanical trituration, and by replating at 5- to 20-fold lower density. For recording purposes, a fraction of cells (~100–200 μl of the cell suspension) were replated on coverslips and placed in 35-mm plastic Petri dishes. Experiments were carried out on those cells, usually 2–48 h after reseeding. All cell culture reagents were purchased from Gibco-Life Technologies (Grand Island, NY).

Electrophysiology

The macroscopic activity of Ca_v3 channels in HEK-293 cells was examined using the whole-cell configuration of the patch-clamp technique (Hamill et al., 1981; Marty & Neher, 1995). Recordings were obtained at room temperature (21–23°C) using an Axopatch 200B amplifier, a Digidata 1322a A/D converter, and pCLAMP 8.02 software (Axon Instruments, Foster City, CA). Data were usually sampled at 5–10 kHz, following 5 kHz analog filtering, except for tail currents, which were digitized at 50 kHz and filtered at 10 kHz. Whole-cell series resistance (initially 3.7 ± 0.3 MΩ, $n = 242$) was estimated from optimal cancellation of the capacitive transients with the built-in circuitry of the amplifier, and was compensated electrically by 60–70%. The average cell capacitance was 20.8 ± 1.4 pF ($n = 242$). The holding potential was −100 mV. In most of the cases, currents were recorded on two channels, one with on-line leak subtraction using the P/−4 method, and the other to evaluate cell stability and holding current. Only leak-subtracted data are shown.

Solutions

Whole-cell Ca^{2+} currents were recorded using the following external solution (in mM): 175 tetraethylammonium (TEA) chloride, 2 $CaCl_2$, and 10 HEPES, pH adjusted to 7.4 with TEA-OH. The internal pipette solution contained the following (in mM): 135 CsCl, 10 EGTA, 2 $CaCl_2$ (free Ca^{2+} ~ 28 nM, calculated with the BAD program), 1 $MgCl_2$, 4 Mg-ATP, 0.3 Na_3GTP, and 10 HEPES, pH adjusted to 7.3 with CsOH. The recording chamber (volume ~0.2 ml) was continuously perfused by gravity at a rate of 1.5–2 ml/min. Bath solution exchange was done by a manually controlled six-way rotary valve. Pipettes were made from TW150−3 capillary tubing (World Precision Instruments, Inc., Sarasota, FL), using a Model P-97 Flaming-Brown pipette puller (Sutter Instrument Co., Novato, CA). Under these solution conditions the pipette resistance was typically 2–3 MΩ.

To investigate the effect of inorganic ions on Ca_v3 channel activity, 100 mM aqueous stock solutions of Cd^{2+}, Ni^{2+} and/or Co^{2+} chloride (Sigma-Aldrich Co, St Louis, MO) were prepared and then diluted with external solution to the required concentration.

Data Analysis

Clampfit 8.0 software (Axon Instruments) was used to obtain peak current values and exponential fits. Dose-response analysis and graphing of the data were done with Prism (GraphPad, San Diego, CA). The following Hill equation was used to fit dose–response data:

$$Y = 1/(1 + 10^{((\mathrm{Log}IC_{50} - X) * h)}) \quad (1)$$

where X is the logarithm of concentration, Y is the fraction of control current remaining after addition of the antagonist, IC_{50} is the concentration causing 50% inhibition of currents, and h is the Hill slope and gives a measure of steepness of the curve. For this analysis, current in control external solution was normalized to 1, and we assumed complete block of current with sufficient concentration of the antagonist. The voltage dependence of activation was estimated using a modified Boltzmann function to fit I-V data:

$$I = I_{max}(V_m - V_{rev})/(1 + \exp((V_{1/2} - V_m)/k)) \quad (2)$$

where I is current, V_m is the test potential, V_{rev} is the apparent reversal potential, $V_{I/2}$ is the mid-point of activation, and k is the slope factor.

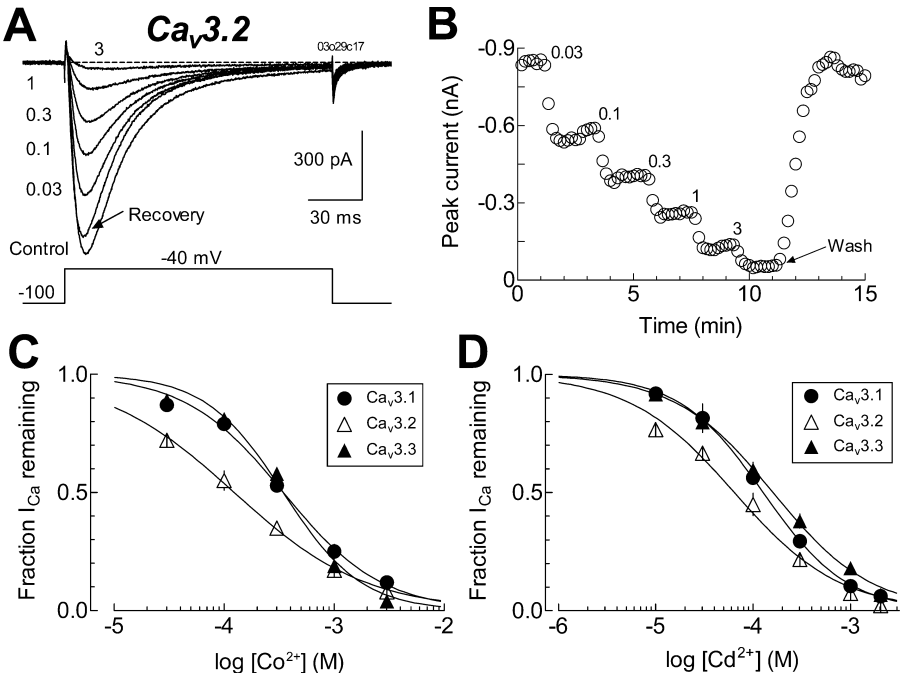

Fig. 1. Human Ca_v3 channel block by the divalents Co^{2+} and Cd^{2+}. Representative traces (*A*) and time course of inhibition (*B*) of $Ca_v3.2$ currents by increasing Cd^{2+} concentrations. Ca^{2+} currents were recorded from an HEK-293 cell stably expressing $Ca_v3.2$ channels in response to depolarizing steps at −40 mV, applied every 10 s. Dose-response relationships of $Ca_v3.1$ (*circles*), $Ca_v3.2$ (*empty triangles*), and $Ca_v3.3$ (*filled triangles*) current block induced by Co^{2+} (*C*) and Cd^{2+} (*D*). The fraction I_{Ca} remaining was calculated considering peak values of control currents and residual currents recorded in the presence of each blocking cation. Data shown (n = 4–7 at each concentration) were fitted with the Hill function (*continuous lines* Eq. 1, *see* Materials and Methods), the parameter obtained are shown in Table 1.

Instantaneous *I–V* relations were analyzed by fitting exponentials to the tail currents generated by repolarization after brief (2–10 ms; *see* Fig. 4) steps to +60 mV, or longer steps to different potentials (*see* Fig. 6). The fit region began once the tail currents reached a peak, usually 0.15–0.35 ms after repolarization, and extended to 15 ms. The amplitude and time constant (τ, tau) obtained with the fittings were used to plot the instantaneous *I–V* relationships and to calculate the percent block of tail amplitude, and to plot the deactivation time constant channels versus the repolarization potential. $Ca_v3.1$ and $Ca_v3.2$ tail currents were well fitted by single exponentials. Only when the blocker accelerated tail currents (e.g., Co^{2+} and Ni^{2+}), they were fitted with two exponentials, where the first tau was fixed to that observed in control conditions and the second tau was not constrained. It has been previously reported that $Ca_v3.3$ tail currents are fit better to two exponentials (Frazier et al., 2001; Gomora et al., 2002). Throughout the present study, $Ca_v3.3$ tail currents were also fitted with the sum of two exponentials. However, in order to simplify the analysis of the inorganic blockers' effects on $Ca_v3.3$ tail currents, here we use the weighted tau ($A_1\tau_1 + A_2\tau_2$; where, A_1 and A_2, are the normalized amplitude of the fast and slow component), which we have previously shown to accurately reflect the voltage dependence of the fast and slow components of $Ca_v3.3$ tail currents (Gomora et al., 2002).

All quantitative results are given as the mean ± SEM. Differences in means were tested with unpaired two-tailed Student's *t*-test and were accepted as significant if $P < 0.5$.

Results

$Ca_v3.2$ Is more Sensitive to Block by Divalent Metals

In this study we investigate the ability of the inorganic ions Cd^{2+} and Co^{2+} to block the cloned human T-type channels: $Ca_v3.1$, $Ca_v3.2$, and $Ca_v3.3$, stably expressed in HEK-293 cells. Using 2 mM Ca^{2+} as charge carrier, the concentration-dependent block by the divalents on T-type channel activity was determined by applying test pulses to −40 mV from a holding potential of −100 mV. Figure 1 shows a typical experiment using an HEK-293 cell expressing $Ca_v3.2$ channels. Representative traces of Ca^{2+} currents obtained in response to increasing concentrations of Co^{2+} are shown in panel *A*, and the time course of block for the same cell is illustrated in panel *B*. Block by Co^{2+}, as well as by Cd^{2+}, was fast and fully reversible. To quantitate the relative potency of these inorganic ions, dose response curves were constructed for both divalents (Cd^{2+} and Co^{2+}) and for each of the T-type channels, after measuring the cumulative block at different concentrations. The respective curves for Co^{2+} and Cd^{2+} are shown in Fig. 1C and *D*, and the parameters obtained by fitting the experimental data with the Hill equation are listed in Table 1. As shown previously for Ni^{2+} (Lee et al., 1999b), $Ca_v3.2$ was also more sensitive to the divalents tested in this study. The concentration at which 50% of $Ca_v3.2$ Ca^{2+} current was blocked (IC_{50}) was 65 and 122 μM for Cd^{2+} and Co^{2+}, respectively (Table 1). The corresponding values for $Ca_v3.1$ and $Ca_v3.3$ were 2–3 times larger for the same divalent metals. Inhibition curves for Cd^{2+} and Co^{2+} had Hill coefficients close to −1 (−0.7 to −1.2), with the smallest values belonging to $Ca_v3.2$ again. Taken together, these results suggest that $Ca_v3.2$ is the most sensitive of the cloned T-type subunits to Cd^{2+} and Co^{2+}.

We next examined the voltage dependence of block for each of the divalents used in this study. To reach this goal, we applied typical *I–V* protocols in

Table 1. Summary of the dose-dependent block by inorganic ions deduced from test pulses to −40 mV

	$Ca_v3.1$		$Ca_v3.2$		$Ca_v3.3$	
	IC_{50}	h	IC_{50}	h	IC_{50}	h
Cd^{2+}	128	−1.0	65	−0.8	157	−0.9
Co^{2+}	335	−0.9	122	−0.7	345	−1.2
Ni^{2+}	250	−1.0	12	−0.8	216	−0.9

[a]Data from Lee et al., 1999b. IC_{50} values are in μM.

the absence, in the presence, and after washout of antagonist concentrations that inhibit the currents by at least 50% (usually slightly above IC_{50} values, *see* Table 1). Figure 2*A* shows current families obtained from an HEK-293 cell expressing $Ca_v3.1$ channels in response to the indicated *I–V* protocol recorded under control, 150 μM Cd^{2+}, and wash-out conditions. Peak current amplitudes were averaged for each experimental condition and plotted as a function of the membrane potential (V_m) for the three Ca_v3 subfamily members (Fig. 2*B*, *C* and *D*, respectively). Inward currents generated from all three recombinant channels started to be detectable at −70 mV, and reached peak near −40. The apparent reversal potential for all channels was $\sim$ +30 mV. The inward currents were carried by Ca^{2+} (2 mM), while the outward currents were carried by Cs^+ (135 mM). Experimental data were fitted with a modified Boltzmann function (*see* Materials and Methods) and the obtained parameters for the different conditions and antagonists of the three α_1 subunits are presented in Table 2. Figure 2*A* shows that Cd^{2+} strongly blocks inward currents, but outward currents were practically unaffected in all three channels (Fig. 2*B*, *C* and *D*). Such behavior was observed also when using Co^{2+} and Ni^{2+} (the latter was used for comparison in some experiments), suggesting that these inorganic ions may be acting as pore-channel blockers. Analysis of results shows that Cd^{2+} did not modify the voltage dependence of current activation of $Ca_v3.1$ and $Ca_v3.3$ channels, but there was a small shift of 3.6 mV to less negative voltages in the $V_{1/2}$ of $Ca_v3.2$. On the contrary, the apparent reversal potential (V_{rev}) was 5.6 and 4.2 mV less positive in the presence of Cd^{2+} with respect to the control condition for $Ca_v3.1$ and $Ca_v3.2$, respectively (Table 2). While for $Ca_v3.3$ channels, a smaller change (2.6 mV) was observed in V_{rev} due to the Cd^{2+} effect. These results suggest that the Cd^{2+} binding site in $Ca_v3.3$ channels might have a slower dissociation rate compared with that of $Ca_v3.1$ and $Ca_v3.2$ channels.

Block by Co^{2+} and Ni^{2+} Is Stronger at Negative Potentials

The blocking effect of Co^{2+} and Ni^{2+} was clearly different from the one induced by Cd^{2+} on Ca_v3 channels. As can be concluded from Table 2, the voltage dependence of $Ca_v3.1$ and $Ca_v3.3$ activation was shifted to more depolarized potentials. The changes in the $V_{1/2}$ values were between 4 and 9 mV, and the biggest shift was observed for $Ca_v3.3$ channels in the presence of Co^{2+} ($V_{1/2}$ −50.0 ± 0.3 mV and −41.2 ± 0.2 mV, for control and Co^{2+} conditions, respectively). Smaller changes, but statistically significant, were observed for $Ca_v3.2$ channels in the presence of Cd^{2+} (3.6 mV shift) and Ni^{2+} (2.6 mV shift) (Table 2). To analyze with more detail these effects, we calculated the percentage block of the peak current at potentials between −60 and +10 mV for each inorganic ion and for the three T-type channels. The results are summarized in Fig. 3, which also illustrates the blocking effect of Cd^{2+} and Co^{2+} on Ca_v3 channel currents recorded at −60 and −20 mV (Fig. 3*A–C*). Generally speaking, $Ca_v3.2$ channel behavior was practically voltage independent in response to the blocking effect of any of the inorganic ions tested in this study (Fig. 3*E*). In addition, unblocking at extreme potentials was practically absent in $Ca_v3.2$ channels (*see* Fig. 5 and 6). On the contrary, $Ca_v3.1$ and $Ca_v3.3$ channels showed a pronounced voltage-dependent block in the presence of Co^{2+} and Ni^{2+}, characterized by stronger block at negative potentials (Fig. 3*D* and *F*). In both channels, block by Co^{2+} inhibited approximately twice the amount of current at −60 mV than at 0 mV. A weaker voltage-dependent effect was also observed for the blocking of $Ca_v3.1$ channels by Cd^{2+} (Fig. 3*D*), however, in this case, the block increases as the membrane potential is more depolarized. The percentage of $Ca_v3.1$ current inhibited goes from 56 ± 3 at −60 mV to 81 ± 6 at +10 mV. These results are consistent with previous reports about the absence of voltage dependence of block of Ni^{2+} on $Ca_v3.2$ currents (Mlinar & Enyeart, 1993c; Lee et al., 1999b), and also with the shift to more positive potentials of the voltage-dependent activation curve of $Ca_v3.1$ channels in the presence of 1 mM Ni^{2+}, but not with 1 mM Cd^{2+} (Lacinova, Klugbauer & Hofmann, 2000). The voltage-dependent block of the current by Co^{2+} and Ni^{2+} was accompanied by modest but significant alterations in current kinetics, mainly for the inactivation and in the range of voltages between −60 to −30 mV. The inactivation time constant was slowed

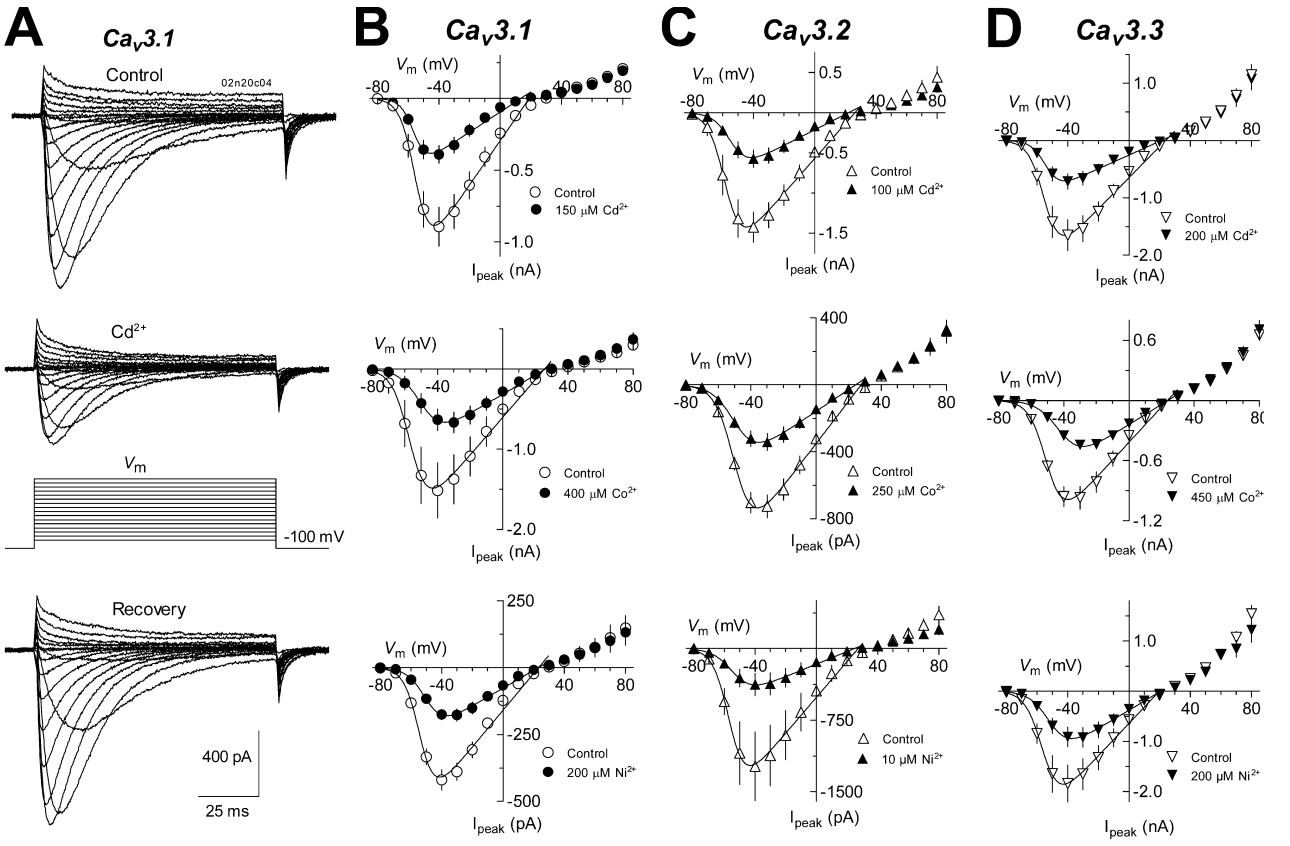

Fig. 2. Effect of Cd^{2+}, Co^{2+}, and Ni^{2+} on Ca_v3 channels' current-voltage relationship. (*A*) Typical family of $Ca_v3.1$ currents shown before (*Control*), in the presence of (Cd^{2+}) and after exposure (*Recovery*) to 150 μM Cd^{2+}. In this cell, such a concentration inhibited peak current at −40 mV by 56%. Currents were activated from −100 mV by voltage steps applied at 0.1 Hz to various test potentials between −80 and +80 mV. Averaged peak currents were plotted against test potential under the indicated experimental conditions and blockers for $Ca_v3.1$ (*B*), $Ca_v3.2$ (*C*) and $Ca_v3.3$ (*D*) channels (n = 4–5). *I–V* data was fitted with a modified with a Boltzmann function (*continuous lines*; Eq. 2, *see* Materials and Methods); the parameters obtained are shown in Table 2. Note that outward currents are poorly affected by the action of the inorganic blocker.

Table 2. Summary of V_{rev} and $V_{1/2}$ data from peak *I–V* fitted curves

		Control		Inorganic blocker		Recovery	
		V_{rev}	$V_{1/2}$	V_{rev}	$V_{1/2}$	V_{rev}	$V_{1/2}$
Cd^{2+}	$Ca_v3.1$	19.0 ± 0.6	−55.0 ± 0.3	13.4 ± 0.8*	−56.1 ± 0.4	18. 8 ± 0.7	−57.8 ± 0.3
	$Ca_v3.2$	26.3 ± 0.8	−57.9 ± 0.4	22.1 ± 0.8*	−54.3 ± 0.5*	25.9 ± 0.8	−59.6 ± 0.3
	$Ca_v3.3$	23.8 ± 0.6	−54.7 ± 0.3	21.2 ± 0.7*	−53.9 ± 0.4	23.0 ± 0.6	−56.6 ± 0.4
Co^{2+}	$Ca_v3.1$	25.7 ± 0.7	−56.3 ± 0.3	26.3 ± 0.5	−49.3 ± 0.3*	23.5 ± 0.8	−59.5 ± 0.4
	$Ca_v3.2$	27.7 ± 0.5	−49.4 ± 0.2	24.3 ± 0.4*	−48.9 ± 0.3	24.2 ± 0.5	−53.6 ± 0.3
	$Ca_v3.3$	23.7 ± 0.6	−50.0 ± 0.3	23.9 ± 0.3	−41.2 ± 0.2*	22.7 ± 0.7	−52.2 ± 0.4
Ni^{2+}	$Ca_v3.1$	23.2 ± 1.1	−53.7 ± 0.6	23.0 ± 0.8	−49.7 ± 0.5*	19.7 ±0.9	−55.1 ± 0.5
	$Ca_v3.2$	27.3 ± 0.7	−56.3 ± 0.3	24.9 ± 0.6*	−53.7 ± 0.4*	25.7 ± 0.8	−61.2 ± 0.4
	$Ca_v3.3$	19.9 ± 0.6	−55.7 ± 0.3	20.9 ± 0.5	−50.7 ± 0.3*	22.0 ± 0.9	−58.1 ± 0.5

Values are in mV. Data are expressed as mean values ± SEM. Statistically significant differences between control and inorganic blocker conditions are noted if the P value was <0.01 (*). The number of cells varies from 3 to 7 for each condition.

down by 25–50% in both channels $Ca_v3.1$ and $Ca_v3.3$; such effect was not observed in $Ca_v3.2$ channels. This effect on current kinetics agrees with the observation that Co^{2+} and Ni^{2+} block was weaker at positive potentials compared with negative voltages (Fig. 3*D* and *F*). Blockers that unblock at positive potentials (e.g., Co^{2+} and Ni^{2+}) would unblock during the test pulse, leading to slower apparent inactivation. On the

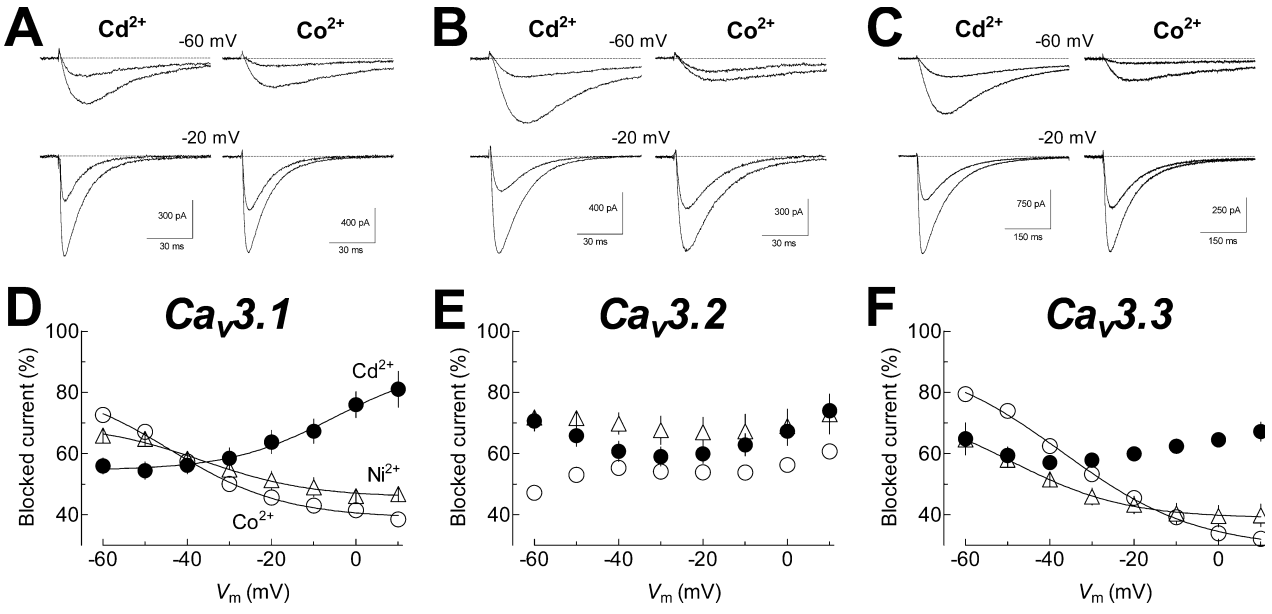

Fig. 3. Voltage-dependent block of Ca_v3 currents by Cd^{2+}, Co^{2+}, and Ni^{2+}. Representative Ca^{2+} currents at −60 (*top traces*) and −20 mV (*bottom traces*) recorded in the absence (*larger currents*) and the presence (*smaller currents*) of Cd^{2+} (*left traces*) and Co^{2+} (*right traces*) for $Ca_v3.1$ (*A*), $Ca_v3.2$ (*B*), and $Ca_v3.3$ (*C*) channels. (*D*)–(*E*). Current recordings obtained under Ni^{2+} conditions showed similar effects to these illustrated for Co^{2+}. Percent block of peak current induced by Cd^{2+} (*filled circles*), Co^{2+} (*empty circles*) and Ni^{2+} (*empty triangles*) as a function of test potential for $Ca_v3.1$ (*D*), $Ca_v3.2$ (*E*) and $Ca_v3.3$ (*F*) channels. Data were obtained from the same cells as in Fig. 2. Continuous lines are spline curves fit to the averaged data to indicate the tendencies of voltage-dependent block.

other hand, Cd^{2+} slightly speeds up the inactivation time constant of $Ca_v3.1$ channels at voltages between −30 to + 20 mV (*data not shown*). In this case, because Cd^{2+} block was more potent at positive potentials (Fig. 3*A* and *D*), then the block would occur during the test pulse, leading to faster inactivation rates (Gomora et al., 2001).

Unblocking of *T*-Type Calcium Channels at Extreme Negative Potentials

In order to further investigate the blocking effect of inorganic ions on T-type cloned channels, we used tail-current protocols to explore the possibility that extreme potentials might relieve channels from block exerted by the antagonists. We first applied a voltage protocol designed to record tail currents at different potentials (repolarization potential) after an activating pulse to + 60 mV for a short period of time (2 ms for $Ca_v3.1$ and $Ca_v3.2$, and 10 ms for $Ca_v3.3$) to minimize inactivation of the channels (Fig. 4*A*). Fig. 4 shows a typical experiment for investigating unblock of $Ca_v3.1$ channels at extreme negative potentials in the presence of Co^{2+}. Representative tail currents recorded at −180, −150, −120, −90, −60 and −30 mV under control, 150 μM Co^{2+} and recovery conditions are illustrated in Fig. 4*A*. Tail current amplitudes for each condition were measured and plotted against the respective repolarization potentials (Fig. 4*B*). Inhibition of the currents by Co^{2+} (or any other inorganic ion) was assessed by applying test pulses to −40 mV for 150 ms (for $Ca_v3.1$ and $Ca_v3.2$) or 500 ms (for $Ca_v3.3$) of duration. As with the *I–V* experiments, we routinely used blocker concentrations slightly above the IC_{50} values to reach a stationary block of ~60–70%. The percentage of block caused by Co^{2+} on $Ca_v3.1$ tail current amplitudes increases sharply with the repolarization at negative potentials (Fig. 4*C*). Data in Fig. 4*C* indicate that the fraction of blocked channels was significantly higher at −180 mV than at −40 mV (85 ± 1% at −180 mV compared with 45 ± 2% at −40 mV). In other words, repolarization at −180 mV induced an additional 40% block of $Ca_v3.1$ channels that were not blocked during the repolarization to −40 mV. Blocking of the channels at negative potentials in the presence of Co^{2+} showed strong voltage dependence in the range of −160 to −20 mV. This effect was also observed with $Ca_v3.3$ and $Ca_v3.2$, although the latter channels were less sensitive to the repolarization effect (Fig. 5). In the presence of Co^{2+}, block of $Ca_v3.2$ channels increased from 51 ± 4% at −20 mV to 67 ± 4% at −180 mV; and for $Ca_v3.3$, from 41 ± 3% to 75 ± 1 % at the same voltages.

We repeated the same experiments described for Co^{2+}, to explore the possible unblocking of T-type channels in the presence of Ni^{2+} and Cd^{2+}. The results are presented in Fig. 5. Panels *A*, *B* and *C* show the data obtained from $Ca_v3.1$, $Ca_v3.2$ and $Ca_v3.2$,

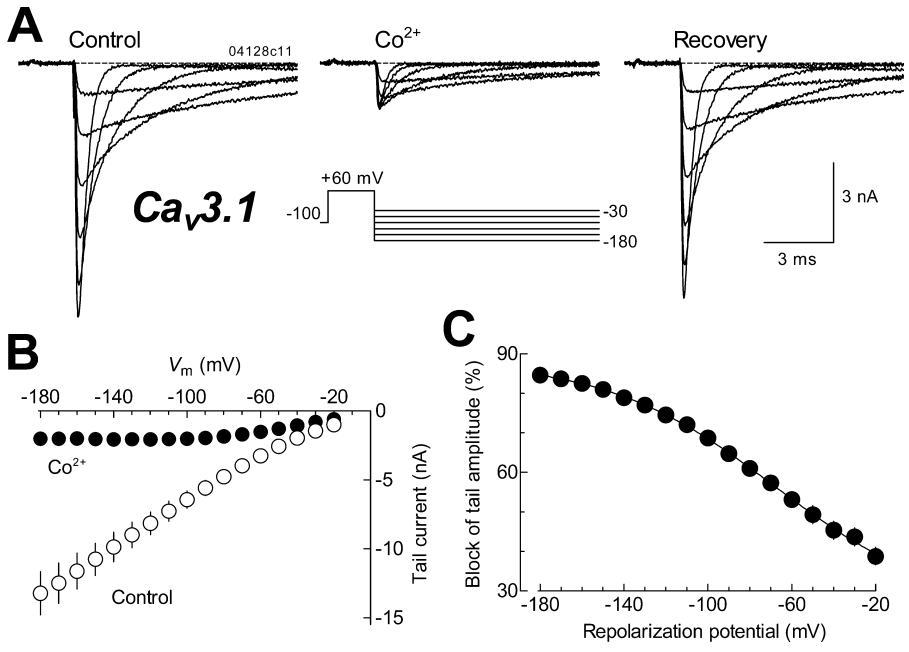

Fig. 4. Extreme negative voltages induce stronger Co^{2+} block on $Ca_v3.1$ channels. (*A*) Representative $Ca_v3.1$ tail currents recorded after repolarization to various membrane potentials before (*Control*), in the presence of (Co^{2+}) and after exposure (Recovery) to 500 μM Co^{2+}. In this cell, such a concentration inhibited peak current at −40 mV by 59%. Shown are tail currents recorded following repolarization to −180, −150, −120, −90, −60 and −30 mV at each experimental condition. A 2-ms step to +60 mV was used to activate channels. Recordings were filtered at 10 kHz and digitally sampled every 20 μs. (*B*) Averaged $Ca_v3.1$ tail current amplitudes ($n = 6$) are plotted versus repolarization potential in the absence (*Control, empty circles*) and in the presence (*Co^{2+}, filled circles*) of 500 μM Co^{2+}. (*C*). Voltage dependence of block by Co^{2+} of tail currents. Percent block of tail amplitudes was calculated from the same data shown in (*B*). Note that block increases as membrane is repolarized to more negative potentials.

respectively. Compared with Co^{2+}, Ni^{2+} had a similar but weaker effect on Ca_v3 channels. However, in the presence of Cd^{2+}, the repolarization to negative potentials evoked a totally distinct behavior of the blocked channels. Cd^{2+} block of $Ca_v3.1$ tail currents decreased considerably at more negative repolarizing steps (Fig. 5*A*). Block of tail currents was always less than that observed during test pulses to −40 mV, however in the presence of Cd^{2+}, this difference was more evident at negative potentials (*compare* Figs. 3 and 5). Data in Fig. 5*A* indicates that the fraction of blocked channels diminished from 50 ± 1% at −40 mV to 26 ± 2% at −180 mV. In other words, repolarization at −180 mV induced the unblocking of 52% of the channels that were blocked at −40 mV. Unblocking of the channels in the presence of Cd^{2+} showed strong voltage dependence in the range of −100 to −20 mV, but at more negative potentials the unblock was almost voltage-independent (26 ± 2% at −180 mV versus 32 ± 2% at −100 mV). Unblock of $Ca_v3.2$ and $Ca_v3.3$ channels under Cd^{2+} conditions had a behavior similar to $Ca_v3.1$, although $Ca_v3.2$ channels showed smaller percentages of unblocking at all the potentials explored (Fig. 5).

Taken together, these results suggest that extreme hyperpolarization appears to attract Cd^{2+} into the cell, allowing Ca^{2+} ions to go through the channel and, therefore, decreasing the percentage of block at negative potentials. In contrast, the binding of Co^{2+} and Ni^{2+} to the blocking site is drastically favored at negative potentials, which results in a higher fraction of blocked channels at those voltages.

Effect of Extreme Depolarizations on Ca_v3 Channel Block by Inorganic Cations

In sympathetic neurons, applying extreme positive potentials transiently relieves block of HVA Ca^{2+} channels by Cd^{2+} (Brown, Tsuda & Wilson, 1983; Thevenod & Jones, 1992). To determine whether block of recombinant human Ca_v3 channels by any of the inorganic ions used in this study may be transiently relieved at positive potentials, we measured tail currents at −100 mV after depolarizing steps to potentials as positive as +120 mV (*see* protocol in Fig. 6*A*). The results are summarized in Fig. 6. Representative recordings obtained from an HEK-293 cell expressing $Ca_v3.3$ channels before, during, and after exposure to 200 μM Cd^{2+}, are shown in panel *A*. Tail currents were generated by repolarization to −100 mV when peak current was reached at each depolarizing potential; as a consequence the duration of each depolarizing step is shorter as it becomes more positive. For clarity, only

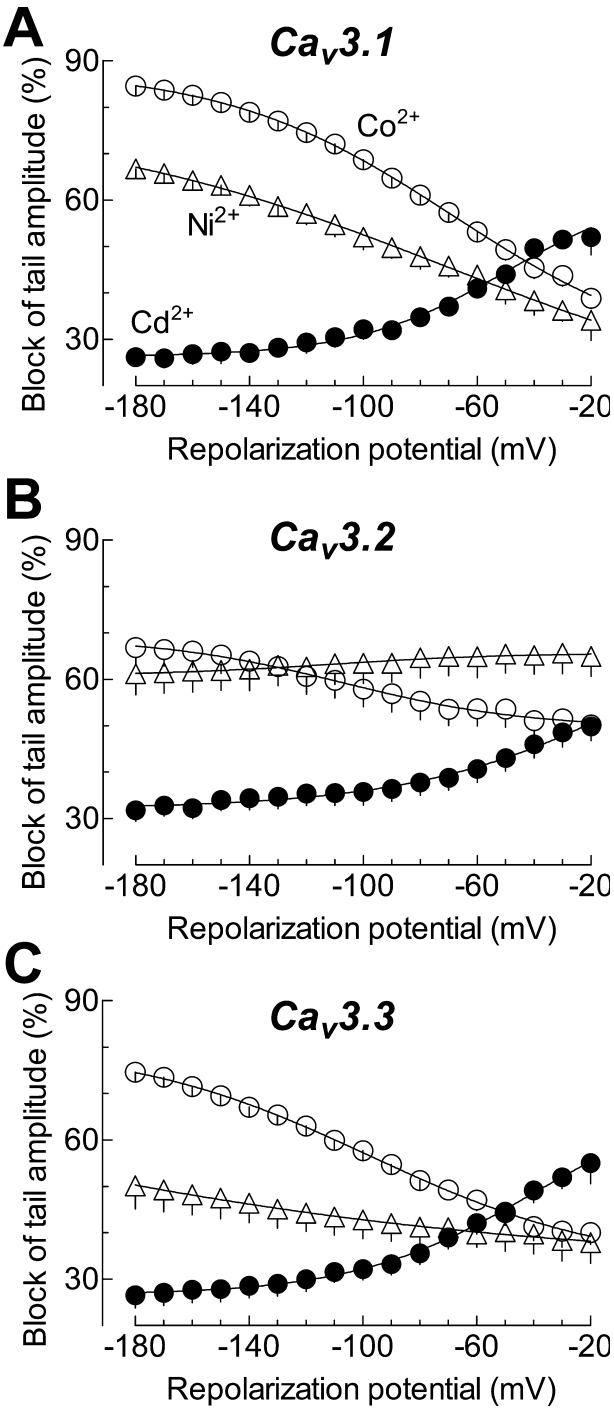

Fig. 5. Effect of extreme negative voltages on blocked Ca_v3 channels by blocking cations. Percent block of tail amplitudes induced by repolarizing to the indicated V_ms in the presence of Cd^{2+} (*filled circles*), Co^{2+} (*empty circles*) and Ni^{2+} (*empty triangles*) for $Ca_v3.1$ (*A*), $Ca_v3.2$ (*B*) and $Ca_v3.3$ (*C*) channels (n = 4–9). Note that extreme negative voltages induced unblocking of Cd^{2+}-blocked channels, while the same voltage protocol increased the amount of channels blocked by Co^{2+} and Ni^{2+}. It can also be observed that the effects on $Ca_v3.2$ channels are much weaker compared with those on $Ca_v3.1$ and $Ca_v3.3$.

8 out of 18 current traces obtained in each condition are shown. Amplitudes of each tail current versus depolarization potential are plotted in Fig. 6*B*. Tail-current amplitudes keep increasing at potentials as positive as +100 mV, which indicates that more $Ca_v3.3$ channels are activated at very positive potentials (Frazier et al., 2001; Gomora et al., 2002). Block by Cd^{2+} did not prevent this peculiarity of $Ca_v3.3$ channels (Fig. 6*B*). Block of tail currents, expressed as percentage, induced by each of the inorganic ions tested for $Ca_v3.1$, $Ca_v3.2$ and $Ca_v3.3$, is shown in Fig. 6*C*, *D* and *E*, respectively. Among the three T-type channels, $Ca_v3.2$ exhibited practically no unblocking at positive potentials. In the presence of Cd^{2+}, all Ca_v3 channels showed 12–19% of unblock after repolarization from negative voltages (−50 to 0 mV); when repolarization was made from positive potentials (from 0 to +120 mV) there was no additional unblocking of the channels (Fig. 6*C–E*). This observation is in agreement with the relief of Cd^{2+} promoted at negative potentials and the observation that outward currents were practically not affected by Cd^{2+}. For instance, in the case of $Ca_v3.3$ channels, while the percentage of current inhibited during test potentials from −50 to 0 mV was very similar (63 ± 3%, *data not shown*), the percentage of inhibition of tail currents did decrease from 57 ± 3 to 42 ± 2% in the same voltage range (Fig. 6*E*). This could be explained by the fact that Cd^{2+} inhibition of outward currents was very weak (Fig. 2), as a consequence tail currents generated after repolarizations from potentials above V_{rev} did not show additional unblocking of Ca_v3 channels. Furthermore, the percentage of blocked current was the same during the pulse (from 18 ± 5% at +60 mV to 20 ± 3% at +120 mV, *data not shown*) as that exhibited by the tail currents (from 34 ± 3% at +60 mV to 33 ± 3% at +120 mV; Fig. 6*E*). Taken together, these results indicated that block of Ca_v3 channels by Cd^{2+} can be transiently relieved at negative potentials, while outward currents are poorly blocked by the divalent.

In contrast, unblocking of $Ca_v3.1$ and $Ca_v3.3$ channels at positive potentials was clearly observed in the presence of Ni^{2+}. Unblocking of these channels in the presence of Co^{2+} was also promoted by extreme depolarizations but the effect was much smaller (Fig. 6*C*, and *E*). Relief of Ni^{2+} block by extreme positive voltages of $Ca_v3.3$ channels has been already documented by Lee et al. (1999b). The results obtained in the present study show that $Ca_v3.1$ channels, but not $Ca_v3.2$, can also be relieved from Ni^{2+} block at positive potentials. The percentages of block of tail amplitudes for $Ca_v3.3$ channels in the presence of Ni^{2+} after repolarizing from −50 and +120 mV were 74 ± 4% and 44 ± 4%, respectively (Fig. 6*E*), which indicates that 40% of the channels blocked at −50 mV were unblocked at +120 mV. The corre-

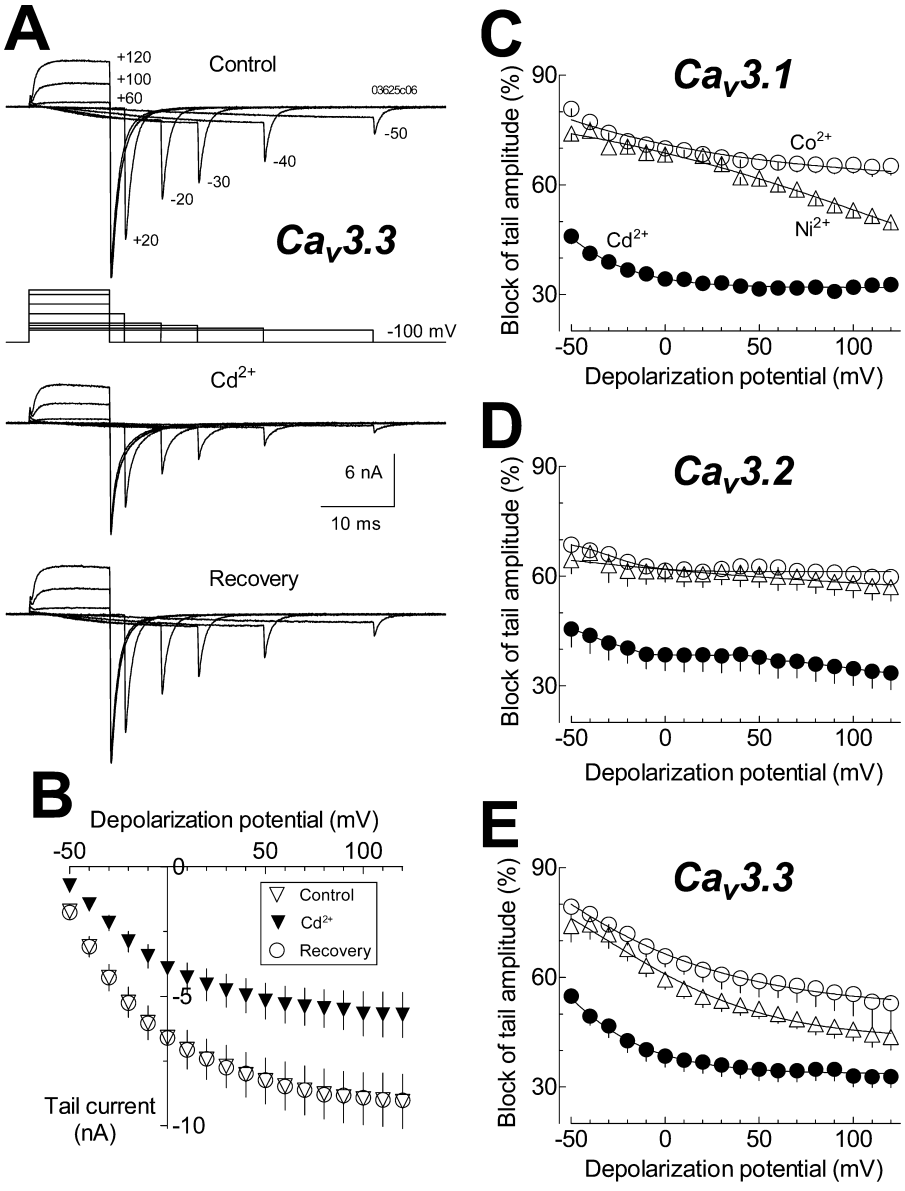

Fig. 6. Strong depolarizations induce partial unblocking in $Ca_v3.1$ and $Ca_v3.3$ channels. (*A*) Representative $Ca_v3.3$ tail currents recorded before (*Control*), in the presence (Cd^{2+}) and after exposure (*Recovery*) to 200 μM Cd^{2+}. In this cell, 200 μM Cd inhibited peak currents evoked at −40 mV by 69%. Tail currents were obtained in response to repolarizations to −100 mV after depolarizing pulses to the indicated potentials. Duration of the depolarizing pulse for each particular voltage was such that the tail current is elicited at the peak of the inward current. Recordings were filtered at 10 kHz and digitally sampled every 20 μs. (*B*) Average $Ca_v3.3$ tail current amplitudes ($n = 14$) obtained with the voltage protocol shown in (*A*) under the indicated experimental conditions. (*C*), (*D*), and (*E*) Percent block of tail current amplitudes for $Ca_v3.1$, $Ca_v3.2$, and $Ca_v3.3$, respectively, induced by the exposure to $\sim IC_{50}$ concentrations of the indicated inorganic blockers. Experimental data points were fitted with spline curves (smooth lines). Note that, again, effects on $Ca_v3.2$ channels are much weaker compared with those on $Ca_v3.1$ and $Ca_v3.3$.

sponding value for $Ca_v3.1$ channels was 30%. In summary, extreme positive potentials are very effective to induce relief of block by Ni^{2+} in $Ca_v3.1$ and $Ca_v3.3$ channels, but much less effective when Co^{2+} or Cd^{2+} is the blocking agent.

Effects on Tail-Current Kinetics

The effect of Co^{2+}, Cd^{2+} and Ni^{2+} on the deactivation kinetics of T-type channels are summarized in Fig. 7. Ca^{2+} tail currents were recorded in response to the protocol already described in Fig. 4*A*. Representative tail currents recorded in control, Ni^{2+} and recovery conditions are illustrated for the three Ca_v3 channels in Fig. 7*A–C*. In the three conditions, tail currents recorded at −100 mV are shown with the exponentials fitted (*dashed thick line*). $Ca_v3.1$ and $Ca_v3.2$ tail currents obtained before and after exposure to Ni^{2+} were well fitted with a single exponential (*Control* and *Recovery* traces), but when tail currents recorded in the presence of the inorganic blocker were fitted with one exponential, a fast component was missed by the fit (Ni^{2+}, upper traces). In order to properly adjust these tails, they were fit better to two exponentials, where the first time constant was constrained to that observed in control (Ni^{2+}, lower traces). The second tau (the faster one) would accurately reflect the (re)blocking of open channels by Ni^{2+}. Re-blocking time constants, together with those of control and recovery conditions, are plotted versus the repolarization potential at which they were recorded for $Ca_v3.1$ and $Ca_v3.2$ channels in Fig. 7*D* and *E*. As can be seen, re-blocking taus were not detectably voltage-dependent for potentials where tail

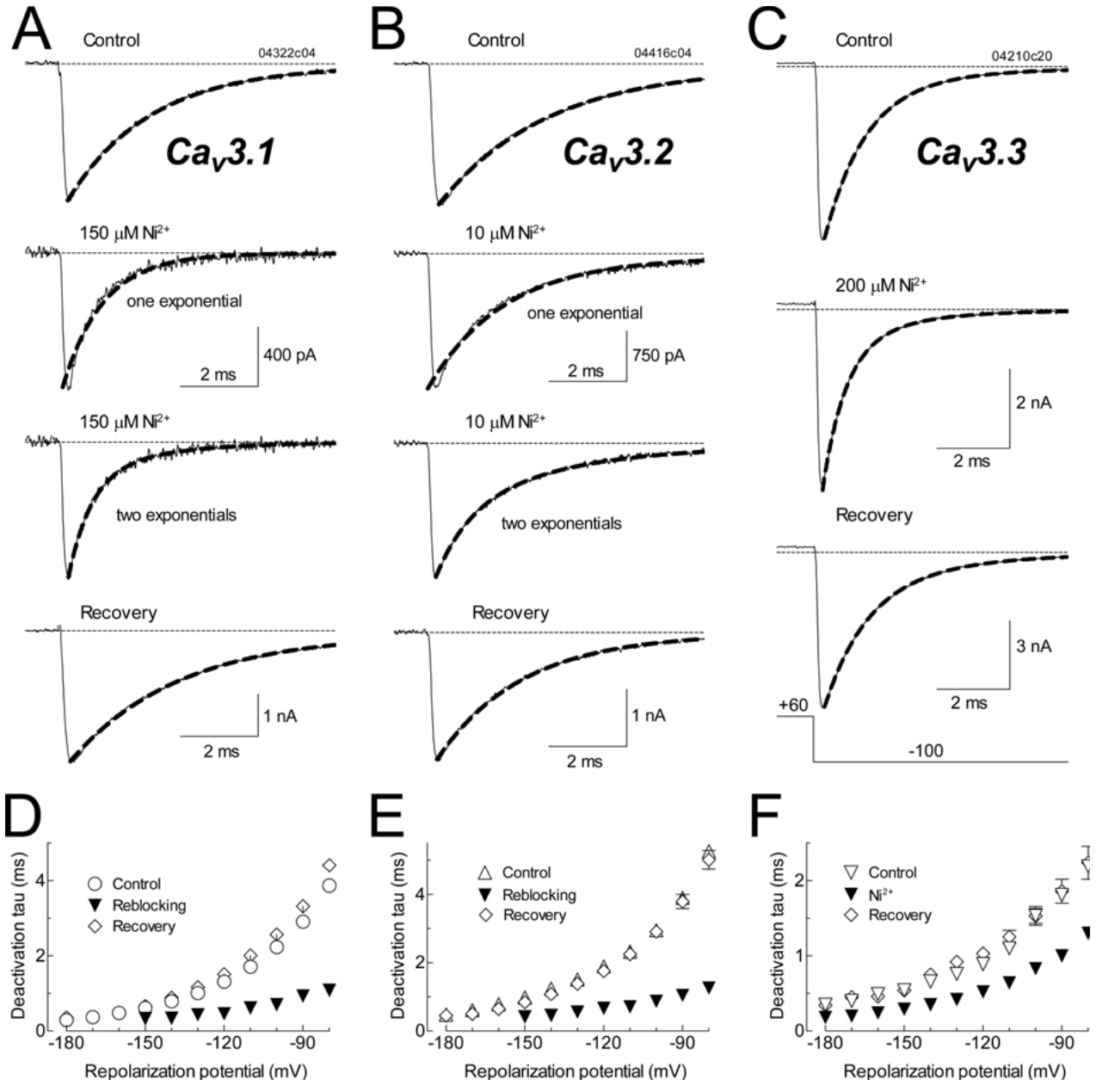

Fig. 7. Acceleration of $Ca_v3.1$ tail currents by Ni^{2+} and Co^{2+}, but not by Cd^{2+}. Representative tail currents obtained from HEK-293 cells stably transfected with $Ca_v3.1$ (*A*), $Ca_v3.2$ (*B*), and $Ca_v3.3$ (*C*) α1 subunits. Shown are tail currents recorded following repolarization to −100 mV after brief depolarization steps to +60 mV in the absence (*Control*), in the presence (Ni^{2+}), and after application (*Recovery*) of the indicated $NiCl_2$ concentrations. In *A* and *B*, thick dashed lines are fits to a single exponential (*Control,* Ni^{2+} upper traces, and *Recovery*), or the sum of two exponentials (Ni^{2+}, lower traces). In *C*, all thick dashed lines are two exponential fits. For clarity, the protocol (illustrated at the bottom in *C*) and recordings show only 0.8 out of 2 ms (for $Ca_v3.1$ and $Ca_v3.2$), and 1 out of 10 ms (for $Ca_v3.3$) of the depolarization at +60 mV, and 8 out of 18 ms of the repolarization. Time constants (tau) for the closing of $Ca_v3.1$ (*D*), $Ca_v3.2$ (*E*), and $Ca_v3.3$ (*F*) channels obtained from exponential fits to tail currents, as explained in *A–C*, recorded at the indicated voltages. In *D* and *E*, reblocking tau values correspond to the second tau fitted to tail currents in the presence of Ni^{2+} (*see* Text). This tau reflects the time course of open channel (re)block by Ni^{2+}. In *F*, all tau values are time constants of the weighted tau (*see* Materials and Methods) calculated from biexponential fits of tail currents recorded under the indicated experimental conditions.

currents reflect mainly closing of the channels (i.e., between −150 and −100 mV). More negative than −150 mV, re-blocking taus are not shown because Ni^{2+} tail currents were fit better with one exponential, as closing-channel and re-blocking taus tend to reach the same value.

Deactivation of $Ca_v3.3$ channels is more complex than in the other two members of the Ca_v3 subfamily.

Table 3. Time constant (τ) values obtained from fitted tail currents

	$Ca_v3.1$			$Ca_v3.2$			$Ca_v3.3$		
	Control	Block	Recovery	Control	Block	Recovery	Control	Block	Recovery
Cd^{2+}									
−120 mV	1.3 ± 0.07 (5)	1.4 ± 0.05	1.4 ± 0.09	1.5 ± 0.08 (7)	1.4 ± 0.04	1.7 ± 0.12	1.0 ± 0.07 (7)	1.6 ± 0.08	1.2 ± 0.05
−100 mV	2.3 ± 0.11	2.2 ± 0.11	2.3 ± 0.17	2.4 ± 0.13	2.1 ± 0.07	2.7 ± 0.09	1.5 ± 0.18	2.1 ± 0.10	1.5 ± 0.20
Co^{2+}									
−120 mV	1.7 ± 0.13 (6)	0.8 ± 0.04	1.7 ± 0.06	1.9 ± 0.32 (5)	0.6 ± 0.11	2.1 ± 0.33	1.2 ± 0.04 (5)	0.7 ± 0.03	1.1 ± 0.07
−100 mV	2.9 ± 0.25	1.3 ± 0.07	2.9 ± 0.08	2.9 ± 0.49	0.7 ± 0.10	3.2 ± 0.46	1.7 ± 0.10	1.1 ± 0.03	1.5 ± 0.11
Ni^{2+}									
−120 mV	1.3 ± 0.11 (6)	0.5 ± 0.04	1.5 ± 0.13	1.9 ± 0.09 (5)	0.7 ± 0.08	1.8 ± 0.17	0.9 ± 0.05 (5)	0.5 ± 0.03	1.1 ± 0.12
−100 mV	2.2 ± 0.21	0.7 ± 0.11	2.6 ± 0.20	2.9 ± 0.22	0.9 ± 0.13	2.9 ± 0.30	1.5 ± 0.22	0.9 ± 0.07	1.6 ± 0.23

Tail currents were fitted with one exponential for $Ca_v3.1$ and $Ca_v3.2$ control and recovery conditions at −120 and −100 mV. For the same channels, values shown in the *Block* columns correspond to the second τ obtained from two exponential fits of tail currents recorded in the presence of the blocker, where the first τ was fixed to that observed in control. $Ca_v3.3$ figures are weighted τ (*see* Materials and Methods) values for each experimental condition. Data are expressed as mean ± SEM. The number of cells is reported in parentheses.

It usually requires two exponentials to properly fit tail currents (Frazier et al., 2001; Gomora et al., 2002). In this study, $Ca_v3.3$ tail current analysis was simplified by fitting two exponentials in the absence and the presence of the inorganic blocker (Fig. 7*C*). For example, at −100 mV, control tail currents decayed with a fast τ of 1.3 ± 0.1 and a slow τ of 6.2 ± 0.9 ms (n = 5). The fast component (A_1) predominates at potentials between −100 and −180 mV, and the slow component (A_2) increases as the repolarizing steps progress to less negative potentials. The A_1 amplitude at −100 mV decreases from 98 ± 2 to 83 ± 3% in the presence of Ni^{2+}, with a consequent increase in A_1. The effects of inorganic blockers on $Ca_v3.3$ tail current kinetics were analyzed by using a weighted τ, which involves the taus and amplitudes of both fitted exponentials to tail currents (*see* Materials and Methods). Figure 7*F* shows weighted τ values obtained from $Ca_v3.3$ tail currents before (*Control*), in the presence (*Ni^{2+}*), and after exposure to 200 μM $NiCl_2$ (*Recovery*). The effect of Ni^{2+} on $Ca_v3.3$ deactivation kinetics was very similar to that observed for $Ca_v3.1$ and $Ca_v3.2$ channels (Fig. 7*D–F*). Tail currents were sped up in the presence of the blocker at the whole range of voltages investigated, which suggests that Ni^{2+} re-blocking is similar among all three Ca_v3 channels.

Analysis of all three Ca_v3 tail currents recorded in the presence of Co^{2+}, but not with Cd^{2+}, produced similar results to those described for Ni^{2+} This is illustrated with the data in Table 3, which shows tau values of fitted tail currents recorded at −120 and −100 mV of all three Ca_v3 channels in the presence and the absence of Cd^{2+}, Co^{2+}, and Ni^{2+}. It can be observed that Cd^{2+} did not change significantly the kinetics of $Ca_v3.1$ and $Ca_v3.2$ tail currents; on the contrary, in the presence of Co^{2+} and Ni^{2+}, deactivation was clearly accelerated at both voltages (*Block* column). As mentioned above, the re-blocking tau reflects the time course of open-channel block by the inorganic blocker. For instance, at −100 mV the time constant for Ni^{2+} re-blocking of $Ca_v3.1$ channels was 0.7 ± 0.1 ms (n = 6), which at this concentration would correspond to a bimolecular association constant of 9.5×10^6 M^{-1} s^{-1}. The corresponding values for Co^{2+} were 1.3 ± 0.07 ms (n = 6), and 1.6×10^6 M^{-1} s^{-1}. The acceleration in the closing time constant observed in tail currents recorded in the presence of Co^{2+} and/or Ni^{2+}, could be reflecting the block of additional channels that were opened, but not blocked, during the test pulse.

As can be seen in Table 3, time constants for the closing of $Ca_v3.1$ and $Ca_v3.2$ channels were practically the same in control and Cd^{2+} conditions. This observation suggests that Cd^{2+} (re)blocking of these channels is instantaneous relative to the speed of our voltage-clamp system (time constant < 60 μs). So, it means that the time constant for reblocking by 150 μM Cd^{2+} is faster than 0.3 ms. This would correspond to a bimolecular blocking rate of $\sim 2.2 \times 10^7$ M^{-1} s^{-1}, which is slightly lower than the one reported in N-type Ca^{2+} channels (10^8 M^{-1} s^{-1}; Thevenod & Jones, 1992), and closer to that obtained from single-channel data of L-type Ca^{2+} channels (4×10^7 M^{-1} s^{-1}; Lansman et al., 1986). To our knowledge, there is no Cd^{2+} data for T-type channels, however, a bimolecular blocking rate of $\sim 10^7$ M^{-1} s^{-1} has been reported for Mg^{2+} in $Ca_v3.1$ channels (Serrano et al., 2000), and 3.7×10^6 M^{-1} s^{-1} for Ni^{2+} in $Ca_v3.3$ (Lee et al., 1999b). All these data suggest that this group of metal divalents binds to Ca^{2+} channels very rapidly (especially Cd^{2+}), essentially diffusion limited.

A totally different Cd^{2+} effect was observed in $Ca_v3.3$ tail currents; in fact, this divalent slowed down the time course of $Ca_v3.3$ channel deactivation (Table 3 and Fig. 8*A*). Interestingly, the effect was

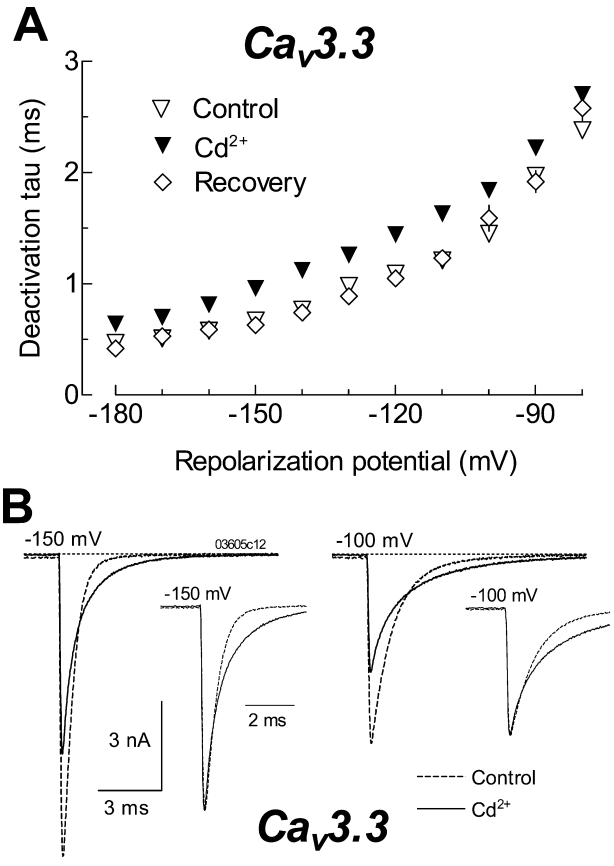

Fig. 8. $Ca_v3.3$ channels close more slowly in the presence of Cd^{2+}. (*A*) Dependence of deactivation time constants on repolarization potential for $Ca_v3.3$ channels before (*Control, empty inverted triangles*), during (*Cd^{2+}, filled inverted triangles*) and after (*Recovery, open diamonds*) exposure to 200 μM Cd^{2+}. Tail currents (recorded as shown in Fig. 7) were fitted with two exponentials beginning 0.35 ms after repolarization from +60 mV. Data points are weighted tau averages of 9 cells. (*B*) Representative tail currents at −150 and −100 mV obtained from a HEK-293 cell stably expressing $Ca_v3.3$ channels in the absence (*Control dashed tail*) and the presence (*Cd^{2+}, continuous tail*) of 200 μM Cd^{2+}. In this cell, such a concentration inhibited peak current at −40 mV by 63%. For clarity, protocol shows only 1.5 out of 10 ms of the depolarization at +60 mV, and 10.5 out of 50 ms of the repolarization. The insets show *Cd^{2+}* tail currents normalized with respect control tail amplitudes, to allow direct comparison of closing time course. Note that tail currents recorded in the presence of Cd^{2+} cross above the control recordings, suggesting that closing of the average channel is delayed until Cd^{2+} leaves the pore of the channel.

limited to the range of voltages where tail currents reflect basically the closing of channels, and the contribution to the tail current from inactivation of channels is practically absent (−180 to −90 mV). The slowing of the time constants shown by $Ca_v3.3$ tail currents indicates quite a different Cd^{2+} effect on the channels. As can be seen in Fig. 8*B*, $Ca_v3.3$ tail currents recorded in the presence of Cd^{2+} cross over with those of control, which suggests that this divalent actually slows down the closing of the channel (confirmed when tails were normalized in amplitude, Fig. 8*B*, *insets*). We further investigated the slowing of $Ca_v3.3$ channel tail currents in the presence of Cd^{2+} by testing the effect of different concentrations of the divalent. Slowing of channel closing was not detected with 30 μM Cd^{2+}, but with 100 μM the effect was already present and it reached saturation with 500–1000 μM of the inorganic ion. For example, time-constant values for closing of $Ca_v3.3$ channels at −120 mV were (in ms): 1.1 ± 0.06 (n = 15), control; 1.0 ± 0.09 (n = 8), 30 μM Cd^{2+}; 1.4 ± 0.12 (n = 7), 100 μM Cd^{2+}; 1.6 ± 0.07 (n = 6), 250 μM Cd^{2+}; 1.8 ± 0.10 (n = 8), 500 μM Cd^{2+}; and 1.8 ± 0.14 (n = 4), 1000 μM Cd^{2+}. Crossing of tail currents was observed at all voltages between −180 to −80 mV. This result indicates that Cd^{2+} in fact slows down the closing of $Ca_v3.3$ channels and suggests that the divalent has to leave the permeation pathway in order for $Ca_v3.3$ channels to close.

Discussion

Block of Ca_v3 Channels by Cd^{2+}, Co^{2+}, and Ni^{2+}

In this study we show that among the three members of T-type channels, $Ca_v3.2$ is the most sensitive to block by the divalents Cd^{2+} and Co^{2+}. Both of these inorganic ions blocked the current through the recombinant T-type channels in a concentration-dependent manner, with a characteristic of 1:1 ligand:receptor binding (Fig. 1 and Table 1). Our observation that inward currents are strongly blocked while outward currents are poorly affected (Fig. 2), agrees with previous results, suggesting that inorganic ions act as pore channel blockers of voltage-dependent Ca^{2+} channels (Swandulla & Armstrong, 1989; Mlinar & Enyeart, 1993; Lee et al., 1999b). In addition, our results show that the mechanism of action of Cd^{2+}, Co^{2+} and Ni^{2+} on T-type channels also includes a voltage dependence of block, which is more prominent in $Ca_v3.1$ and $Ca_v3.3$ currents (Figs. 3 and 5). More interestingly, Co^{2+} and Ni^{2+} share some block properties, stronger inhibition of currents at negative voltages and speeding up of tail currents, while Cd^{2+} block is characterized by exerting the opposite effects. Our findings also show that $Ca_v3.3$ channels can not close when Cd^{2+} is in the permeation pathway.

Previous studies have also shown a preferential block of other divalents on $Ca_v3.2$ channels (Lee et al., 1999b; Jeong et al., 2003). The differential selectivity found in the present study among the T-type channels is not as has been described for Ni^{2+} and Zn^{2+}, so far the antagonists with the best blocking potency for discriminating among T-type channels. Combining our results with those of previous studies, the inhibitory effect of divalent

inorganic cations on recombinant T-type channels is as follows: $Cu^{2+} > Zn^{2+} > Ni^{2+} > Cd^{2+} > Co^{2+}$; this sequence applies to the three members of T-type channels, with $Ca_v3.2$ channels more sensitive than $Ca_v3.1$ and $Ca_v3.3$. As a consequence of our results, La^{3+} and the lanthanides remain the most potent blockers of T-type channels at nanomolar concentrations (Biagi & Enyeart, 1990; Mlinar & Enyeart, 1993; Beedle et al., 2002; Obejero-Paz et al., 2004).

The IC_{50} values (Table 1) indicate that Ni^{2+} is a better blocker than Cd^{2+} for LVA channels, but only when currents are carried by $Ca_v3.2$ channels; in the other two members of the LVA subfamily, Cd^{2+} seems to be slightly more potent than Ni^{2+}. Several neuronal and non-neuronal preparations show similar order of potency ($Cd^{2+} > Ni^{2+}$; Akaike et al., 1989; Akaike, Kostyuk & Osipchuk, 1989; Takahashi & Akaike, 1991; Herrington & Lingle, 1992; Lacinova et al., 2000). However, other studies (that include neurons, cardiac and endocrine cells) have found that LVA currents are blocked more potently by Ni^{2+} than by Cd^{2+}; in such preparations, Ca_v3 .2 channels may contribute significantly to the total T-type current (Kaneda & Akaike, 1989; Wu & Lipsius, 1990; Arnoult, Villaz & Florman, 1998; Talley et al., 1999; Perchenet, Benardeau & Ertel, 2000; Schrier et al., 2001).

Unblocking at Extreme Potentials

Unblocking of HVA Ca^{2+} channels at extreme positive and negative voltages in the presence of Cd^{2+} has been reported in sympathetic and sensory neurons (Jones & Marks, 1989; Swandulla & Armstrong, 1989; Thevenod & Jones, 1992). LVA channel unblock by inorganic ions has been less explored. In one study, Mlinar & Enyeart (1993) used human and rat C cells, where LVA Ca^{2+} current (~90% of total I_{Ca}) seems to be carried by $Ca_v3.2$ channels based on its sensitivity to Ni^{2+}. They did not find any significant unblocking at extreme positive potentials when using La^{3+}, Y^{3+} or Ni^{2+} to block T-type tail currents. In a more recent study, using recombinant $Ca_v3.3$ channels and Ni^{2+} as antagonist, a fractional unblocking of these channels after depolarizations to positive voltages was reported (Lee et al., 1999b). In the present work, we analyzed for the first time the effects of extreme potentials on the block of all three Ca_v3 channels by Cd^{2+}, Co^{2+} and Ni^{2+}, and we found that the blocking mechanism of these inorganic ions is related to their ionic radii and also to the specific T-type channel isoform. First, we found Co^{2+} and Ni^{2+} effects to be very similar, i.e., block was voltage-dependent with stronger inhibition of the current at negative potentials (Fig. 3), which results in a shift of the *I–V* relationship to more negative potentials (Table 2). In addition, repolarization to extreme negative voltages (up to −180 mV) increases sharply the fraction of blocked channels (Fig. 5). These effects were selective for $Ca_v3.1$ and $Ca_v3.3$ channels; the only exception was a small fractional unblocking of $Ca_v3.2$ channels observed in the presence of Co^{2+} (about one third of that observed for the other two T-type channels, Fig. 5*B*). Second, the voltage-dependent effects of Cd^{2+} were opposite to those shown by Co^{2+} and Ni^{2+}. Cadmium block was slightly enhanced with increasing depolarizations in the physiological range (−60 to +20 mV, mainly for $Ca_v3.1$ channels; Fig. 3*A*), and blocked channels were partially cleared from Cd^{2+} with extreme hyperpolarizations (more negative than −100 mV). Evidence for opposite effects of Cd^{2+} and Co^{2+} on HVA Ca^{2+} channels were shown previously on snail neurons, where a voltage-dependent relief of Cd^{2+} block was seen in tail currents, but after Co^{2+} replacement for Cd^{2+}, the tail currents were practically abolished (Brown et al., 1983). Furthermore, a voltage-independent effect of Ni^{2+} and Co^{2+} has been described in neuronal HVA Ca^{2+} currents (McFarlane & Gilly, 1998; Magistretti, Brevi & de Curtis, 2001; Castelli et al., 2003), although results obtained with recombinant HVA channels showed voltage-dependent effects when Ba^{2+} was the charge carrier (Zamponi, Bourinet & Snutch, 1996). The molecular basis of the distinct mechanism of block by these inorganic ions on HVA and LVA channels remains to be determined.

Cobalt and nickel have very similar ionic radii (0.74 and 0.72 Å, respectively), which is considerably smaller than Cd^{2+} and Ca^{2+} itself (0.97 and 0.99 Å, respectively). So, it can be suggested that small cations (e.g., Co^{2+} and Ni^{2+}) block Ca_v3 channels in a voltage-dependent manner because they are driven deep into the channel pore (without escaping into the cell) at extreme negative potentials, increasing the fraction of channels blocked. The relief of channel block is promoted at positive voltages, as a result of increasing positive charges in the intracellular side of the channel, which expels the positively charged blocker to the extracellular space. On the basis of this interpretation, we can predict that divalent cations like Cu^{2+} and Zn^{2+} (with ionic radii of 0.73 and 0.74 Å, respectively), which strongly block recombinant T-type channels at low micromolar concentrations (Jeong et al., 2003), will show effects similar to those described for Co^{2+} and Ni^{2+} in this work. In brief, the stronger block induced by Co^{2+} and Ni^{2+}, and even by Cd^{2+}, on $Ca_v3.1$ and $Ca_v3.3$ than in $Ca_v3.2$ channel activity, suggests important structural differences in the binding site of these divalents in the pore of T-type channels.

In contrast, block of T-type channels by bigger divalent cations like Cd^{2+} (Fig. 5), can be relieved with repolarizations to extreme negative potentials (more negative than −100 mV), although the block at intermediate voltages shows weak voltage depen-

dence (Fig. 2). Depolarizations to potentials more positive than +50 mV did not produce any relief of Ca_v3 channel block by Cd^{2+} (Fig. 6). There is no data on T-type channels to compare our Cd^{2+} results with, although in HVA channels strong unblocking at extreme positive and negative potentials has been reported (Jones & Marks, 1989; Swandulla & Armstrong, 1989; Thevenod & Jones, 1992; Wakamori et al., 1998). This suggests that the basic mechanism of Cd^{2+} block might be conserved among calcium channels. Several previous studies have established that inorganic Ca^{2+} channel blockers compete with permeant ions for a common high-affinity binding site in the channel pore (Hagiwara & Takahashi, 1967; Swandulla & Armstrong, 1989; Chow, 1991; Kim et al., 1993; Tang et al., 1993; Yang et al., 1993). In this context, the bimolecular blocking rates determined in the present study for Cd^{2+}, Co^{2+} and Ni^{2+} (essentially diffusion-limited) suggest that the blocking ions can easily reach the high-affinity site from the extracellular side of the membrane. This implies that the high-affinity site is located at the external mouth of the Ca_v3 channel's pore.

Despite similarities between HVA and T-type channels regarding the mechanism of block by divalents, especially for Cd^{2+}, we found an intriguing difference between the two major subfamilies of Ca^{2+} channels, and even more among T-type channels themselves. Tail current analysis showed that in $Ca_v3.3$ channels, Cd^{2+} tail currents cross above the control, which is usually interpreted as a significant slowing down of channel closing by the blocker (Chow, 1991; Swandulla & Armstrong, 1989). We found that crossing of tail currents was dependent on Cd^{2+} concentration, requiring 30 μM to be detectable and reaching saturation at 250–500 μM. This suggests that Cd^{2+} is binding to a site within the ion permeation pathway, causing the closing of the channel to be delayed until Cd^{2+} leaves the permeation pathway. It is particularly noteworthy that despite the high level of sequence conservation among Ca_v3 channels in their pore regions (Perez-Reyes, 2003), only $Ca_v3.3$ channel closing was delayed by Cd^{2+}. It is possible, however, that structural differences due to small changes in the sequences might explain the Cd^{2+} effects on $Ca_v3.3$ tail currents. In fact, the differential sensitivity shown by T-type channels to the block by Ni^{2+} (Lee et al., 1999b), might be due to such structural differences as well.

We are deeply grateful to Dr. Edward Perez-Reyes (University of Virginia, Charlottesville, VA) for his enormous contribution providing cell lines stably expressing Ca_v3 channels, and his comments on the manuscript. This work was supported by the following grants: CONACyT (Mexico) I37976-B and J-40693-Q to J.C. Gomora, and DGAPA-UNAM (Mexico) IN201602 to J.C. Gomora.

References

Akaike, N., Kanaide, H., Kuga, T., Nakamura, M., Sadoshima, J., Tomoike, H. 1989. Low-voltage-activated calcium current in rat aorta smooth muscle cells in primary culture. *J. Physiol.* **416:**141–160

Akaike, N., Kostyuk, P.O., Osipchuk, Y.V. 1989. Dihydropyridine-sensitive low-threshold calcium channels in isolated rat hypothalamic neurones. *J. Physiol.* **412:**181–195

Arnoult, C., Villaz, M., Florman, H.M. 1998. Pharmacological properties of the T-type Ca^{2+} current of mouse spermatogenic cells. *Mol. Pharmacol.* **53:**1104–1111

Beedle, A.M., Hamid, J., Zamponi, G.W. 2002. Inhibition of transiently expressed low- and high-voltage-activated calcium channels by trivalent metal cations. *J. Membrane Biol.* **187:**225–238

Biagi, B.A., Enyeart, J.J. 1990. Gadolinium blocks low- and high-threshold calcium currents in pituitary cells. *Am. J. Physiol.* **259:**C515–C520

Bootman, M.D., Lipp, P., Berridge, M.J. 2001. The organisation and functions of local Ca^{2+} signals. *J. Cell Sci.* **114:**2213–2222

Brown, A.M., Tsuda, Y., Wilson, D.L. 1983. A description of activation and conduction in calcium channels based on tail and turn-on current measurements in the snail. *J. Physiol.* **344:**549–583

Castelli, L., Tanzi, F., Taglietti, V., Magistretti, J. 2003. Cu^{2+}, Co^{2+}, and Mn^{2+} modify the gating kinetics of high-voltage-activated Ca^{2+} channels in rat palaeocortical neurons. *J. Membrane Biol.* **195:**121–136

Chow, R.H. 1991. Cadmium block of squid calcium currents. Macroscopic data and a kinetic model. *J. Gen. Physiol.* **98:**751–770

Cribbs, L.L., Gomora, J.C., Daud, A.N., Lee, J.H., Perez-Reyes, E. 2000. Molecular cloning and functional expression of Ca(v)3.1c, a T-type calcium channel from human brain. *FEBS Lett.* **466:**54–58

Cribbs, L.L., Lee, J.H., Yang, J., Satin, J., Zhang, Y., Daud, A., Barclay, J., Williamson, M.P., Fox, M., Rees, M., Perez-Reyes, E. 1998. Cloning and characterization of alpha1H from human heart, a member of the T-type Ca^{2+} channel gene family. *Circ. Res.* **83:**103–109

Elinder, F., Arhem, P. 2003. Metal ion effects on ion channel gating. *Q. Rev. Biophys.* **36:**373–427

Frazier, C.J., Serrano, J.R., George, E.G., Yu, X., Viswanathan, A., Perez-Reyes, E., Jones, S.W. 2001. Gating kinetics of the alpha1I T-type calcium channel. *J. Gen. Physiol.* **118:**457–470

Gomora, J.C., Daud, A.N., Weiergraber, M., Perez-Reyes, E. 2001. Block of cloned human T-type calcium channels by succinimide antiepileptic drugs. *Mol. Pharmacol.* **60:**1121–1132

Gomora, J.C., Murbartian, J., Arias, J.M., Lee, J.H., Perez-Reyes, E. 2002. Cloning and expression of the human T-type channel Ca(v)3.3: insights into prepulse facilitation. *Biophys. J.* **83:**229–241

Hagiwara, S., Takahashi, K. 1967. Surface density of calcium ions and calcium spikes in the barnacle muscle fiber membrane. *J. Gen. Physiol.* **50:**583–601

Hamill, O.P., Marty, A., Neher, E., Sakmann, B., Sigworth, F.J. 1981. Improved patch-clamp techniques for high-resolution current recording from cells and cell-free membrane patches. *Pfluegers Arch.* **391:**85–100

Herrington, J., Lingle, C.J. 1992. Kinetic and pharmacological properties of low voltage-activated Ca^{2+} current in rat clonal (GH3) pituitary cells. *J. Neurophysiol.* **68:**213–232

Jeong, S.W., Park, E.G., Park, J.Y., Lee, J.W., Lee, J.H. 2003. Divalent metals differentially block cloned T-type calcium channels. *Neuroreport* **14:**1537–1540

Jones, S.W., Marks, T.N. 1989. Calcium currents in bullfrog sympathetic neurons. I. Activation kinetics and pharmacology. *J. Gen. Physiol.* **94:**151–167

Kaneda, M., Akaike, N. 1989. The low-threshold Ca current in isolated amygdaloid neurons in the rat. *Brain Res.* **497:**187–190

Kim, M.S., Morii, T., Sun, L.X., Imoto, K., Mori, Y. 1993. Structural determinants of ion selectivity in brain calcium channel. *FEBS Lett.* **318:**145–148

Kim, D., Song, I., Keum, S., Lee, T., Jeong, M.J., Kim, S.S., McEnery, M.W., Shin, H.S. 2001. Lack of the burst firing of thalamocortical relay neurons and resistance to absence seizures in mice lacking alpha (1G) T-type Ca^{2+} channels. *Neuron* **31:**35–45

Lacinova, L., Klugbauer, N., Hofmann, F. 2000. Regulation of the calcium channel alpha (1G) subunit by divalent cations and organic blockers. *Neuropharmacology* **39:**1254–1266

Lansman, J.B., Hess, P., Tsien, R.W. 1986. Blockade of current through single Cd^{2+}, Mg^{2+}, and Ca^{2+} Voltage and concentration dependence of calcium entry into the pore. *J. Gen. Physiol* **88:**321–347

Lee, J.H., Daud, A.N., Cribbs, L.L., Lacerda, A.E., Pereverzev, A., Klockner, U., Schneider, T., Perez-Reyes, E. 1999a. Cloning and expression of a novel member of the low voltage-activated T-type calcium channel family. *J. Neurosci.* **19:**1912–1921

Lee, J.H., Gomora, J.C., Cribbs, L.L., Perez-Reyes, E. 1999b. Nickel block of three cloned T-type calcium channels: low concentrations selectively block alpha1H. *Biophys. J.* **77:**3034–3042

Magistretti, J., Brevi, S., de Curtis, M. 2001. Ni^{2+} slows the activation kinetics of high-voltage-activated Ca^{2+} currents in cortical neurons: evidence for a mechanism of action independent of channel-pore block. *J. Membrane Biol.* **179:** 243–262

Marty, A., Neher., E. 1995. Tight-seal whole-cell recording. *In:* Sakmann, B., Neher, E., (eds) Single Channel Recording. Plenum Press, New York

McFarlane, M.B., Gilly, W.F. 1998. State-dependent nickel block of a high-voltage-activated neuronal calcium channel. *J. Neurophysiol.* **80:**1678–1685

Mitterdorfer, J., Grabner, M., Kraus, R.L., Hering, S., Prinz, H., Glossmann, H., Striessnig, J. 1998. Molecular basis of drug interaction with L-type-Ca^{2+} channels. *J. Bioenerg. Biomembr.* **30:**319–334

Mlinar, B., Enyeart, J.J. 1993a. Block of current through T-type calcium channels by trivalent metal cations and nickel in neural rat and human cells. *J. Physiol.* **469:**639–652

Nachshen, D.A. 1984. Selectivity of the Ca binding site in synaptosome Ca channels. Inhibition of Ca influx by multivalent metal cations. *J. Gen. Physiol.* **83:**941–967

Obejero-Paz, C.A., Gray, I.P., Jones, S.W. 2004. Y^{3+} Block demonstrates an intracellular activation gate for the {alpha} 1G T-type Ca^{2+} channel. *J. Gen. Physiol.* **124:**631–640

Perchenet, L., Benardeau, A., Ertel, E.A. 2000. Pharmacological properties of Ca(V)3.2, a low voltage-activated Ca^{2+} channel cloned from human heart. *Naunyn Schmiedebergs Arch. Pharmacol.* **361:**590–599

Perez-Reyes, E. 2003. Molecular physiology of low-voltage-activated t-type calcium channels. *Physiol. Rev.* **83:**117–161

Perez-Reyes, E., Cribbs, L.L., Daud, A., Lacerda, A.E., Barclay, J., Williamson, M.P., Fox, M., Rees, M., Lee, J.H. 1998. Molecular characterization of a neuronal low-voltage-activated T-type calcium channel. *Nature* **391:**896–900

Schrier, A.D., Wang, H., Talley, E.M., Perez-Reyes, E., Barrett, P.Q. 2001. alpha1H T-type Ca^{2+} channel is the predominant subtype expressed in bovine and rat zona glomerulosa. *Am. J. Physiol* **280:**C265–C272

Serrano, J.R., Dashti, S.R., Perez-Reyes, E., Jones, S.W. 2000. Mg^{2+} block unmasks Ca^{2+}/Ba^{2+} selectively of alpha1G T-type calcium channels. *Biophys. J.* **79:**3052–3062

Swandulla, D., Armstrong, C.M. 1989. Calcium channel block by cadmium in chicken sensory neurons. *Proc. Natl. Acad. Sci. USA* **86:**1736–1740

Takahashi, K., Akaike, N. 1991. Calcium antagonist effects on low-threshold (T-type) calcium current in rat isolated hippocampal CA1 pyramidal neurons. *J. Pharmacol. Exp. Ther.* **256:**169–175

Talley, E.M., Cribbs, L.L., Lee, J.H., Daud, A., Perez-Reyes, E., Bayliss, D.A. 1999. Differential distribution of three members of a gene family encoding low voltage-activated (T-type) calcium channels. *J. Neurosci.* **19:**1895–1911

Tang, S., Mikala, G., Bahinski, A., Yatani, A., Varadi, G., Schwartz, A. 1993. Molecular localization of ion selectivity sites within the pore of a human L-type cardiac calcium channel. *J. Biol. Chem.* **268:**13026–13029

Thevenod, F., Jones, S.W. 1992. Cadmium block of calcium current in frog sympathetic neurons. *Biophys. J.* **63:**162–168

Todorovic, S.M., Jevtovic-Todorovic, V., Mennerick, S., Perez-Reyes, E., Zorumski, C.F. 2001a. Ca(v)3.2 channel is a molecular substrate for inhibition of T-type calcium currents in rat sensory neurons by nitrous oxide. *Mol Pharmacol.* **60:**603–610

Todorovic, S.M., Jevtovic-Todorovic, V., Meyenburg, A., Mennerick, S., Perez-Reyes, E., Romano, C., Olney, J.W., Zorumski, C.F. 2001b. Redox modulation of T-type calcium channels in rat peripheral nociceptors. *Neuron* **31:**75–85

Wakamori, M., Strobeck, M., Niidome, T., Teramoto, T., Imoto, K., Mori, Y. 1998. Functional characterization of ion permeation pathway in the N-type Ca^{2+} channel. *J. Neurophysiol.* **79:**622–634

Wu, J.Y., Lipsius, S.L. 1990. Effects of extracellular Mg^{2+} on T- and L-type Ca^{2+} currents in single atrial myocytes. *Am. J. Physiol.* **259:**H1842–H1850

Yang, J., Ellinor, P.T., Sather, W.A., Zhang, J.F., Tsien, R.W. 1993. Molecular determinants of Ca^{2+} selectivity and ion permeation in L-type Ca^{2+} channels. *Nature* **366:**158–161

Zamponi, G.W., Bourinet, E., Snutch, T.P. 1996. Nickel block of a family of neuronal calcium channels: subtype- and subunit-dependent action at multiple sites. *J. Membrane Biol.* **151:**77–90